The B1-subunit of the H^+ ATPase is required for maximal urinary acidification

Karin E. Finberg*, Carsten A. Wagner[†‡], Matthew A. Bailey[†§], Teodor G. Păunescu[¶], Sylvie Breton[¶], Dennis Brown[¶], Gerhard Giebisch[†], John P. Geibel[†‖], and Richard P. Lifton*[,**††]

Departments of *Genetics, [†]Cellular and Molecular Physiology, [‖]Surgery, and **Howard Hughes Medical Institute, Yale University School of Medicine, New Haven, CT 06510; [¶]Program in Membrane Biology and Renal Unit, Massachusetts General Hospital and Harvard Medical School, Boston, MA 02114; [‡]Institute of Physiology, University of Zurich, Zurich, Switzerland; and [§]Molecular Physiology, University of Edinburgh, Edinburgh, United Kingdom

Contributed by Richard P. Lifton, August 5, 2005

The multisubunit vacuolar-type H^+ATPases mediate acidification of various intracellular organelles and in some tissues mediate H^+ secretion across the plasma membrane. Mutations in the B1-subunit of the apical H^+ATPase that secretes protons in the distal nephron cause distal renal tubular acidosis in humans, a condition characterized by metabolic acidosis with an inappropriately alkaline urine. To examine the detailed cellular and organismal physiology resulting from this mutation, we have generated mice deficient in the B1-subunit (*Atp6v1b1*$^{-/-}$ mice). Urine pH is more alkaline and metabolic acidosis is more severe in *Atp6v1b1*$^{-/-}$ mice after oral acid challenge, demonstrating a failure of normal urinary acidification. In *Atp6v1b1*$^{-/-}$ mice, the normal urinary acidification induced by a lumen-negative potential in response to furosemide infusion is abolished. After an acute intracellular acidification, Na^+-independent pH recovery rates of individual *Atp6v1b1*$^{-/-}$ intercalated cells of the cortical collecting duct are markedly reduced and show no further decrease after treatment with the selective H^+ATPase inhibitor concanamycin. Apical expression of the alternative B-subunit isoform, B2, is increased in *Atp6v1b1*$^{-/-}$ medulla and colocalizes with the H^+ATPase E-subunit; however, the greater severity of metabolic acidosis in *Atp6v1b1*$^{-/-}$ mice after oral acid challenge indicates that the B2-subunit cannot fully functionally compensate for the loss of B1. Our results indicate that the B1 isoform is the major B-subunit isoform that incorporates into functional, plasma membrane H^+ATPases in intercalated cells of the cortical collecting duct and is required for maximal urinary acidification.

collecting duct | intercalated cell | pH homeostasis | renal tubular acidosis | vacuolar H^+ ATPase

Most biological functions, ranging from enzymatic activities to changes in protein conformation that underlie signaling, critically depend on pH. As a consequence, systemic pH is tightly regulated; in humans, for example, the pH of arterial plasma rarely varies from 7.40 under normal circumstances. This tight regulation requires maintenance and replenishment of bicarbonate, the major buffer in plasma, and elimination of acid produced by catabolism. Oxidation of organic compounds produces acid in two forms: the volatile gas CO_2 (which equilibrates with carbonic acid), and nonvolatile acids, such as sulfuric acid, arising from oxidation of sulfur-containing amino acids. Whereas CO_2 is eliminated by gas exchange in the lungs, the latter acids must be eliminated by renal H^+ secretion. In humans, this requires secretion of $\approx$1 meq of H^+ per kg of body weight per day (1). The importance of this secretory mechanism is revealed by distal renal tubular acidosis (dRTA), a disease in which this process is impaired. Affected subjects have marked metabolic acidosis, with arterial pH typically $\approx$7.2, and growth retardation due to leaching of calcium from bones, resulting in rickets, osteomalacia, and the development of renal calcium deposits (nephrocalcinosis) and/or tubular precipitates (nephrolithiasis) (2).

A number of potential mediators underlying this renal proton secretion have been identified (3). These include apical ATP-dependent H^+ pumps and H^+–K^+ATPases on epithelial cells in the distal nephron; in addition, proton secretion is coupled to bicarbonate reabsorption mediated by the Cl^-/HCO_3^- exchanger AE1. Human genetic studies have recently identified essential elements for pH homeostasis. To date, three genes in which mutations cause distal renal tubular acidosis have been identified (4–6). One of these genes, *AE1*, is essential for normal renal bicarbonate reabsorption. The other two genes encode subunits of the vacuolar-type H^+ ATPase expressed in the apical plasma membrane of type A intercalated cells (ICs) of the collecting duct (CD); this H^+ pump mediates secretion of protons into tubular fluid and can support a 1,000-fold concentration gradient (7, 8). Vacuolar-type H^+ ATPases are homologous to the ATP synthase of the inner mitochondrial membrane and are composed of at least 13 subunits (9). These multisubunit complexes are believed to mediate acidification of intracellular compartments in all eukaryotic cells, whereas, in a subset of tissues, including the renal collecting duct, they mediate proton export from cells at the plasma membrane (8, 9). Some H^+ ATPase subunits show specific isoforms that are largely restricted in their cellular localization (10). For example, the B2-subunit is largely found in intracellular compartments (11–14). In contrast, the B1- and a4-subunits, the subunits found mutated in renal tubular acidosis, each show specificity for the plasma membrane H^+ ATPase (6, 11–14), and patients with homozygous loss of function mutations show systemic acidosis due to an inability to produce an appropriately acidic urine (5, 6).

Although these human genetic studies have demonstrated the essential role of the apical H^+ ATPase in normal pH homeostasis, it is extremely difficult to study detailed aspects of nephron function in patients harboring specific mutations. However, these functions can be more fully investigated in animal models of human disease. Accordingly, we have engineered mice deficient for the H^+ ATPase B1-subunit (*Atp6v1b1*$^{-/-}$ mice) and have examined the detailed cellular and organismal physiology resulting from this mutation.

Methods

Generation of *Atp6v1b1*-Deficient Mice. Segments of the 129/SvJ murine *Atp6v1b1* genomic locus (13) were subcloned into Scrambler NTKV-1907 (Stratagene), replacing exons 7–11 with the *Neo* cassette. The 5′ arm and 3′ arms contained 8.3 and 1.7 kb of homology to the genomic locus, respectively. Linearized targeting vector was introduced into CJ7 mouse ES cells by electroporation. Genomic DNA from clones surviving double selection with G418 and ganciclovir was screened for a 2.1-kb

Abbreviations: dRTA, distal renal tubular acidosis; IC, intercalated cell; CD, collecting duct; pH_i, intracellular pH; IM, inner medulla.

[††]To whom correspondence should be addressed at: Yale University School of Medicine, 1 Gilbert Street, TAC S341, New Haven, CT 06520. E-mail: richard.lifton@yale.edu.

PCR amplification product specific for the targeted *Atp6v1b1* locus; the forward primer was specific for the *Neo* cassette, and the reverse primer was specific for an *Atp6v1b1* 3′ flanking sequence not included within the targeting vector. Homologous recombination was confirmed by Southern blotting of HindIII- and EcoRI-digested ES cell DNA with *Atp6v1b1* intron 1 and 3′ flanking region probes, respectively.

Karyotypically normal targeted clones were injected into blastocysts to obtain chimeric mice, which were crossed with C57B/6 females to achieve germ-line transmission of the targeted allele in heterozygous, and ultimately homozygous, animals. Mice were genotyped by PCR using primer pairs specific for the wild-type (WT) (intron/exon 9) and deleted alleles (*Neo* cassette) and genomic DNA as template. *Atp6v1b1*$^{-/-}$ mice derived from two independent targeted ES cell clones were phenotypically indistinguishable. ES cell manipulations were performed by the Transgenic Mouse and Gene Targeting Resource of Yale University.

Animal Care and Diet. Mice were maintained on a standard rodent diet (Prolab RMH3000, LabDiet) with free access to tap water, unless otherwise indicated. For acid-loading studies, a solution of 1.5% (280 mM) NH_4Cl/1% sucrose was substituted for tap water. All procedures were approved by the Yale University Animal Care and Use Committee or the Massachusetts General Hospital Institutional Committee on Research Animal Use.

Western Blotting. Whole mouse kidneys were homogenized in buffer containing protease inhibitors and centrifuged for 15 min at 13,000 × *g* at 4°C to yield total kidney extract. SDS/PAGE (30 μg of total protein per lane) and immunoblotting using a rabbit H^+ ATPase B1-subunit polyclonal antibody (1:1,000) (14) and horseradish peroxidase-conjugated donkey anti-rabbit IgG (1:5,000, Jackson ImmunoResearch) was performed as described (14).

Immunohistochemistry and Histology. After vascular rinsing with PBS, mouse kidneys were fixed with paraformaldehyde–lysine–periodate by intracardiac perfusion of 6-week-old mice, and cryosections (5 μm) were prepared and immunostained (14, 15). Primary antibodies were rabbit polyclonal anti-H^+ ATPase B1-subunit (1:150) (13); rabbit affinity-purified anti-H^+ ATPase B2-subunit (1:10) (14); chicken affinity-purified anti-H^+ ATPase E-subunit (1:100) (16); rabbit affinity-purified anti-AE1 (1:300, Chemicon); rabbit anti-pendrin (1:300, provided by Peter Aronson, Yale University); goat affinity-purified anti-aquaporin 2 (1:100, Santa Cruz Biotechnology). Donkey secondary antibodies were anti-rabbit IgG-Cy3 (1:1,000), anti-goat IgG-Cy5 (1:100), and anti-chicken IgG-FITC (1:60, Jackson ImmunoResearch). Sections (at least two animals per genotype) were imaged by confocal microscopy. Formalin-fixed renal sections from 10-month-old mice were stained with haematoxylin and eosin or van Kossa stain for assessment of histology and calcium phosphate deposition.

Biochemical Analysis and Physical Parameters. Venous blood obtained from the retroorbital plexus of conscious mice (2–3 months old) was immediately analyzed for blood gases and pH; electrolytes and creatinine were measured in the Yale–New Haven Hospital Clinical Chemistry Laboratory. Arterial blood of anesthetized mice (≥5 months old) was analyzed for K^+ levels by flame photometry (17). Urine samples from 3- to 4-month-old mice were collected on Parafilm, and pH was measured by using a glass pH electrode. Urinary calcium levels and osmolality were determined by routine methods. Twenty-four-hour urine output was collected under oil from pairs of 6- to 8-week-old mice housed in metabolic cages (Nalgene), after 3-day adaptation to the cage. Assessments of body weight and of femoral bone density by using a PIXImus Mouse Densitometer (GE Medical Systems) were made on 9-week-old mice. Comparisons of biochemical parameters between groups were made by using the Mann–Whitney Wilcoxon rank sum test for two independent variables. P values <0.05 were considered statistically significant.

Surgical Methods. Renal clearance studies of adult mice (≥5 months old) were conducted by modifying a previous protocol (17). Saline (140 mM NaCl/5 mM KCl) was infused at 0.15 ml/h per 10 g of body weight; after 1.5 h of equilibration, urine output was collected under equilibrated mineral oil for a 30-min control period followed by bolus i.v. injection of furosemide (2 mg/kg) and collection of urine for a second 30-min period. Blood samples (30 μl) were taken immediately before and 1 h after furosemide infusion. Urine electrolytes and pH were measured and compared between genotypes by ANOVA with repeated measures. Comparisons of values within the same genotype before and after the administration of furosemide were made by using a least significant difference test (CSS STATISTICA software). P values <0.05 were considered statistically significant.

Single Tubule Preparation and pH Measurements. Single cortical CD fragments of 6-week-old mouse kidneys were selected under microscopic examination after collagenase digestion by morphologic criteria as described (18). Fragments were mounted in a perfusion chamber and acidified by using the NH_4Cl (20 mM) prepulse technique, and intracellular pH (pH_i) of single ICs was monitored by using the pH-sensitive dye BCECF as described (19). Groups were compared by using the unpaired Student t test. P values <0.05 were considered statistically significant.

Results

Generation of Atp6v1b1$^{-/-}$ Mice. The murine *Atp6v1b1* genomic locus in CJ7 ES cells was disrupted by replacing exons 7–11 with a neomycin resistance cassette via homologous recombination (Fig. 1*a*). Because missense mutations in these exons are sufficient to eliminate normal gene product function, their deletion is anticipated to do the same. Screening of ES cell DNA of 211 clones surviving selection with G418 and gancyclovir identified two clones that yielded a PCR amplification product specific for the targeted *Atp6v1b1* genomic locus (data not shown; see *Methods*). Homologous recombination of both arms of the targeting vector was confirmed in these clones by Southern blotting (Fig. 1 *b* and *c*).

Targeted clones were injected into blastocysts to generate *Atp6v1b1*$^{+/-}$ chimeric mice; chimeric males were, in turn, bred with C57B/6 females. Tail DNAs of the resulting agouti offspring were screened by PCR (see *Methods*) to identify germ-line transmission of the mutant allele, and lines established from both ES clones transmitted the disrupted allele. Intercrossing of *Atp6v1b1*$^{+/-}$ mice yielded offspring of all three genotypes (Fig. 1*d*) in expected Mendelian ratios; there was no evidence for decreased fetal or neonatal viability of *Atp6v1b1*$^{-/-}$ mice. *Atp6v1b1*$^{-/-}$ mice raised on a standard diet were fully fertile and showed normal growth and behavior when followed up to 1 year of age.

Western blotting showed that B1-subunit expression was absent in whole kidney homogenates of *Atp6v1b1*$^{-/-}$ mice (Fig. 1*e*). Immunohistochemistry of kidneys of littermates showed that, whereas the B1-subunit was detected and indistinguishable in ICs of both *Atp6v1b1*$^{+/+}$ (Fig. 2*a*) and *Atp6v1b1*$^{+/-}$ mice (data not shown), it was absent in *Atp6v1b1*$^{-/-}$ mice (Fig. 2*b*). These results confirm that the targeted disruption eliminates production of the normal B1-subunit.

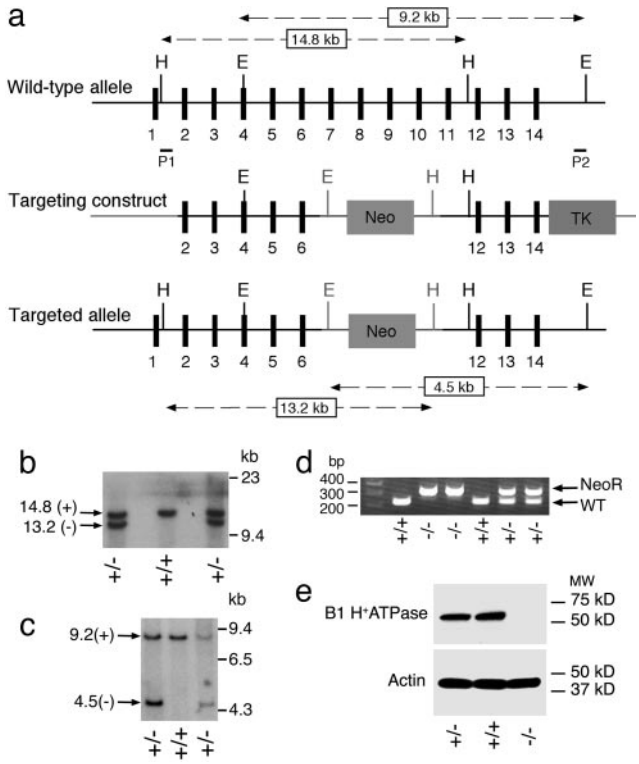

Fig. 1. Generation of H^+ ATPase B1-subunit deficient mice. (*a*) Structure of the endogenous locus, targeting construct and targeted allele are shown. The segments not endogenous to the WT allele are shown in gray. Numbered boxes represent exons of *Atp6v1b1*. The sizes of restriction fragments resulting from HindIII (H) and EcoRI (E) digestion of the WT and targeted alleles, and the locations of probes (P1, P2) used for Southern blotting are shown. ''Neo'' denotes neomycin resistance gene; ''TK'' denotes thymidine kinase gene. (*b* and *c*) Confirmation of *Atp6v1b1* gene targeting. Genomic DNA of WT (+/+) or heterozygous (+/−) targeted deletion ES cell lines were digested with indicated enzymes, fractionated on 0.8% agarose gels, and subjected to Southern blotting. (*b*) Hybridization of probe P1 to HindIII-digested DNA is shown. (*c*) Hybridization of probe P2 to EcoRI-digested DNA is shown. Fragments corresponding to the targeted (−) alleles are seen only in targeted clones. (*d*) Genotyping of *Atp6v1b1* in +/+, +/−, and −/− mice. PCR of genomic DNA was performed by using primer pairs specific for the WT (intron/exon 9) and deleted alleles (Neo cassette) and genomic DNA as template (see *Methods*). Products were resolved on a 2% agarose gel. The inferred genotypes are indicated. (*e*) Immunoblotting of total kidney homogenates with antibodies to the B1-subunit was performed (see *Methods*). Expression is seen in *Atp6v1b1*$^{+/+}$ and *Atp6v1b1*$^{+/-}$ mice, but is absent in *Atp6v1b1*$^{-/-}$ mice.

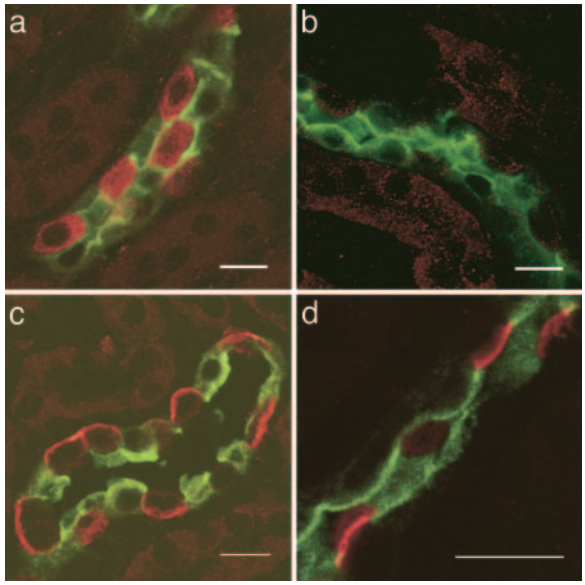

Fig. 2. Immunolocalization of CD cell type-specific markers in WT and *Atp6v1b1*$^{-/-}$ kidney. Renal sections were prepared, stained, and imaged as described in *Methods*. (*a*) Distribution of Atp6v1b1 in WT outer medullary collecting duct (OMCD). CD segments are identified by staining of principal cells with aquaporin-2 (AQP-2, in green); Atp6v1b1 is stained in red, and localizes to intercalated cells (ICs). (*b*) Staining of OMCD from *Atp6v1b1*$^{-/-}$ mouse was performed as in *a*. Architecture of the nephron segment appears normal, but Atp6v1b1 staining is absent. (*c*) Presence of A-ICs in *Atp6v1b1*$^{-/-}$ kidney. Sections were stained for AQP2 (green) and AE1 (red). AE1 staining is present and localizes to the basolateral membrane of ICs of the OMCD, a normal distribution like that seen in WT (not shown). (*d*) Presence of B-ICs in *Atp6v1b1*$^{-/-}$ kidney. Pendrin immunoreactivity (a B-IC marker, red) is detected in an apical distribution in subset of cortical CD cells. This intracellular distribution is similar to that seen in WT (not shown). (Scale bars, 16 μm.)

Cellular Organization of the Collecting Duct in Atp6v1b1$^{-/-}$ Mice. Renal histology of 10-month-old *Atp6v1b1*$^{-/-}$ mice appeared grossly normal with no evidence of nephrocalcinosis (data not shown). To assess renal CD epithelial cell subtype differentiation, we examined the expression of proteins that are normally found in specific cell types. The collecting duct is normally composed of type A ICs (A-ICs), which mediate proton secretion and bicarbonate reabsorption, type B ICs (B-ICs), which mediate bicarbonate secretion, and principal cells, which mediate electrogenic Na^+ reabsorption. These cells are marked by anion exchanger 1 (AE1) on the basolateral membrane, pendrin on the apical membrane, and aquaporin 2 on the apical membrane, respectively. Each of these proteins was present and targeted to its normal subcellular location in kidneys of the *Atp6v1b1*$^{-/-}$ mice (Fig. 2 *c* and *d*). These results suggest that differentiation of the collecting duct epithelia persists in *Atp6v1b1*$^{-/-}$ mice.

Biochemical Parameters on a Standard Diet. The cardinal feature of humans with homozygous loss of *ATP6V1B1* is systemic acidosis with an inappropriately alkaline urine. Among mice fed a standard rodent diet, there was no significant difference in venous pH or plasma bicarbonate level between *Atp6v1b1*$^{+/+}$ and *Atp6v1b1*$^{-/-}$ mice (Fig. 3 *a* and *b* and Table 1). Nonetheless, urine pH was significantly higher among *Atp6v1b1*$^{-/-}$ mice compared to *Atp6v1b1*$^{+/+}$ controls (pH 7.2 vs. 6.1, respectively, $P = 0.0001$; Fig. 3*c* and Table 1), indicating that the B1-subunit normally contributes to the acidic urinary pH.

Other plasma electrolytes showed no significant difference between *Atp6v1b1*$^{+/+}$ and *Atp6v1b1*$^{-/-}$ mice, although *Atp6v1b1*$^{-/-}$ mice showed a trend toward lower potassium levels; similarly, there was no significant difference between genotypes in mean arterial blood pressure, hematocrit, and glomerular filtration rate (Table 1). Compared to WT, there was reduced urine osmolality in *Atp6v1b1*$^{-/-}$ mice ($P = 0.03$) and a trend toward greater 24-h urine output (Table 1). In contrast to the marked hypercalciuria seen in humans, urinary Ca^{2+}/Cr ratios were not elevated, and were in fact significantly reduced in *Atp6v1b1*$^{-/-}$ mice compared to WT ($P = 0.002$; Table 1). Bone densities of *Atp6v1b1*$^{+/+}$ and *Atp6v1b1*$^{-/-}$ mice were not significantly different (Table 1).

Impaired Handling of an Acid Load in Atp6v1b1$^{-/-}$ Mice. The difference in typical diets of mice and humans might account for the absence of systemic acidosis in *Atp6v1b1*$^{-/-}$ mice. To determine whether the mutant mice can secrete an acid load, blood and urinary measurements were compared in *Atp6v1b1*$^{+/+}$ and *Atp6v1b1*$^{-/-}$ mice after acid loading by administration of 1.5% (280 mM) NH_4Cl/1% sucrose in the drinking water. Although this acid load induced a significant reduction in systemic pH in both genotypes, acidosis was significantly more severe in *Atp6v1b1*$^{-/-}$ mice

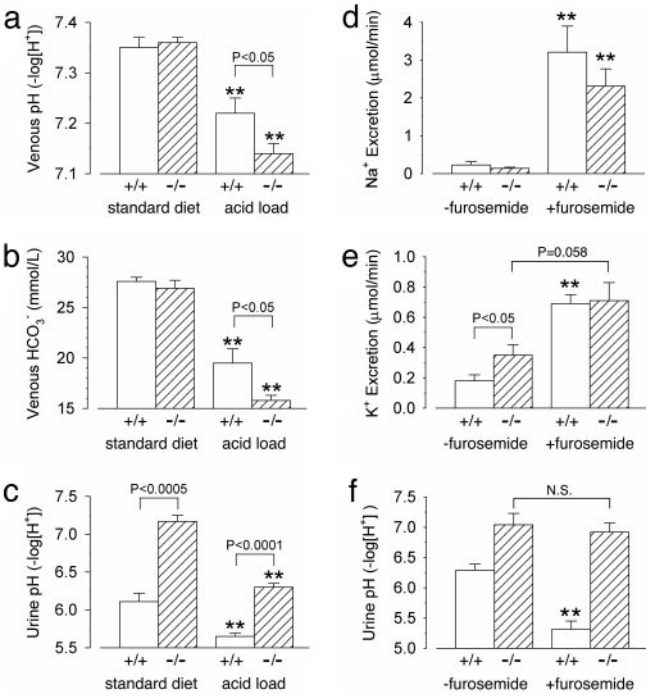

Fig. 3. Defective renal H^+ secretion in *Atp6v1b1*$^{-/-}$ mice. Values in *Atp6v1b1*$^{+/+}$ and *Atp6v1b1*$^{-/-}$ littermates are compared and represented as means ± SE. (*a–c*) Venous pH, plasma HCO_3^- and urine pH were measured on a standard rodent diet with free access to either tap water (standard diet) or a 1.5% NH_4Cl/1% sucrose solution (acid load) (see *Methods*). n = 6–12 mice per genotype. **, $P < 0.001$ standard diet vs. acid load. (*a*) Venous pH. The −/− mice have significantly lower venous pH after acid loading. (*b*) Venous plasma HCO_3^-. The −/− mice have significantly lower plasma HCO_3^- after acid loading. (*c*) Urine pH. Despite lower plasma pH, the −/− mice have higher urine pH, indicating a defect in renal acidification. (*d–f*) Sodium excretion, potassium excretion, and urinary pH were measured in *Atp6v1b1*$^{+/+}$ (n = 9) and *Atp6v1b1*$^{-/-}$ (n = 9) mice before and after i.v. administration of furosemide as described in *Methods*. **, $P < 0.01$, without furosemide vs. with furosemide. (*d*) Sodium excretion. Furosemide dramatically increased natriuresis to a similar degree (P = 0.10) in both +/+ and −/− mice. (*e*) Potassium excretion. Furosemide induced potent kaliuresis to a similar degree in both +/+ and −/− mice (P = 0.337). (*f*) Urine pH. Furosemide induced a marked reduction in urine pH in +/+ mice but no significant change in −/− mice.

(systemic pH 7.22 in WT vs. 7.13 in *Atp6v1b1*$^{-/-}$; $P = 0.036$; Fig. 3*a*). This increased acidosis in *Atp6v1b1*$^{-/-}$ mice was accompanied by a significant reduction in venous plasma bicarbonate level in *Atp6v1b1*$^{-/-}$ mice (19 vs. 16 mmol/liter; $P = 0.036$; Fig. 3*b*). This increased systemic acidosis is accompanied by a failure of *Atp6v1b1*$^{-/-}$ mice to appropriately acidify the urine: despite having a lower systemic pH, these mice have a markedly more alkaline urine (pH 5.7 in WT vs. 6.4 in *Atp6v1b1*$^{-/-}$, $P = 0.0001$; Fig. 3*c*), corresponding to an 80% reduction in free proton concentration. This finding demonstrates that the B1-subunit is essential for achieving maximal urinary acidification. Urinary and venous pH levels at baseline and following acid challenge were not different between *Atp6v1b1*$^{+/-}$ and *Atp6v1b1*$^{+/+}$ littermates (data not shown).

Electrogenic H^+ Secretion in the CD Depends on the B1-Subunit. The above experiment provoked H^+ secretion by increasing the blood concentration of H^+. One can also provoke H^+ secretion acutely by increasing the lumen-negative potential of the collecting duct, which increases the electrical driving force for H^+ secretion. This increase was achieved by i.v. administration of furosemide to anesthetized *Atp6v1b1*$^{+/+}$ and *Atp6v1b1*$^{-/-}$ mice (see *Methods*). Furosemide inhibits NaCl reabsorption in the thick ascending limb of Henle's loop, resulting in a marked natriuresis, which induces a compensatory increase in electrogenic Na^+ reabsorption in the CD via the epithelial Na^+ channel ENaC. This reabsorption increases the lumen-negative potential in the CD, thereby increasing the electrogenic driving force for H^+ secretion (20).

Furosemide induced marked natriuresis in both genotypes; although there was slightly less natriuresis in the *Atp6v1b1*$^{-/-}$ mice, this difference was not significant (Fig. 3*d*). Consistent with an increase in electrogenic driving force in the CD, furosemide induced marked and indistinguishable kaliuresis in both genotypes (Fig. 3*e*). In contrast, whereas furosemide induced a marked increase in urinary acidification in WT mice (10-fold increase in H^+ concentration), there was no significant acidification in *Atp6v1b1*$^{-/-}$ mice (Fig. 3*f*). This finding demonstrates that the normal urinary acidification induced by a lumen-negative potential depends on the presence of functional B1-subunit.

Table 1. Physiological parameters of *Atp6v1b1*$^{-/-}$ mice

	Atp6v1b1$^{+/+}$ (n)	*Atp6v1b1*$^{-/-}$ (n)	P value
Blood			
Na^+, mM	148 ± 0.6 (13)	147 ± 0.4 (13)	NS
K^+, mM	4.22 ± 0.11 (9)	3.90 ± 0.14 (9)	0.077
Cl^-, mM	111 ± 0.9 (13)	110 ± 0.4 (13)	NS
HCO_3^-, mM	27.6 ± 0.4 (6)	26.9 ± 0.8 (6)	NS
Ca^{2+}, mg/dl	10.4 ± 0.1 (13)	10.3 ± 0.1 (13)	NS
Mg^{2+}, mg/dl	2.0 ± 0.04 (9)	2.0 ± 0.09 (8)	NS
PO_4^-, mg/dl	7.1 ± 0.3 (9)	6.9 ± 0.3 (9)	NS
Cr, mg/dl	0.4 ± 0.01 (9)	0.4 ± 0.01 (9)	NS
pH, pH units	7.35 ± 0.02 (6)	7.36 ± 0.01 (6)	NS
GFR, ml/min/100 g	0.71 ± 0.07 (9)	0.77 ± 0.09 (9)	NS
Hematocrit, %	45.9 ± 0.6 (9)	44.0 ± 1.4 (9)	NS
MAP, mmHg	103 ± 4 (9)	98 ± 3 (9)	NS
Urine			
pH, pH units	6.11 ± 0.11 (10)	7.17 ± 0.08 (7)	0.0001
Osm, mmol/kg	1,793 ± 155 (6)	1,248 ± 139 (6)	0.0260
Ca^{2+}/Cr, mg/g	63.1 ± 6.3 (6)	33.1 ± 2.3 (8)	0.0027
Output/pair/d, ml	2.8 ± 0.4 (7)	4.2 ± 0.5 (7)	0.053
Physical parameters			
Body weight, g	23.9 ± 0.6 (8)	24.5 ± 0.8 (8)	NS
Bone density, mg/cm^2	82 ± 2 (8)	81 ± 4 (8)	NS

Values are mean ± SE. GFR, glomerular filtration rate; MAP, mean arterial blood pressure; Cr, creatinine; NS, not significant.

Impaired Proton Extrusion from Intercalated Cells After Intracellular Acidification. To directly examine H^+ efflux from individual ICs, cortical CD fragments were isolated. The ability of single ICs within these fragments to extrude H^+ was measured after acute intracellular acidification induced by exposure to 20 mM NH_4Cl (Fig. 4 *a* and *b*). H^+ extrusion was assessed by monitoring recovery of pH_i with the pH-sensitive dye BCECF (see *Methods*) in the presence and absence of 100 nM concanamycin (CON), a specific inhibitor of the vacuolar-type H^+ ATPases (21), which include the apical H^+ ATPase. In WT mice, mean pH_i recovery rate was reduced ≈70% by CON (Fig. 4*c*; 0.035 ± 0.001 vs. 0.009 ± 0.001 pH units/min), suggesting that this fraction of H^+ efflux is mediated by the activity of plasma membrane H^+ ATPases. The rate of pH_i recovery in *Atp6v1b1*$^{-/-}$ ICs (0.011 ± 0.001 pH units/min) was markedly reduced compared to WT (Fig. 4*c*, mean rate of pH recovery reduced by 70%; $P < 0.001$). In contrast to WT, there was no further reduction in mean recovery of *Atp6v1b1*$^{-/-}$ cells after addition of CON (0.009 ± 0.001 pH units/min; Fig. 4*c*). These results demonstrate that normal H^+ excretion after acute intracellular acidification requires H^+ ATPases containing the B1-subunit.

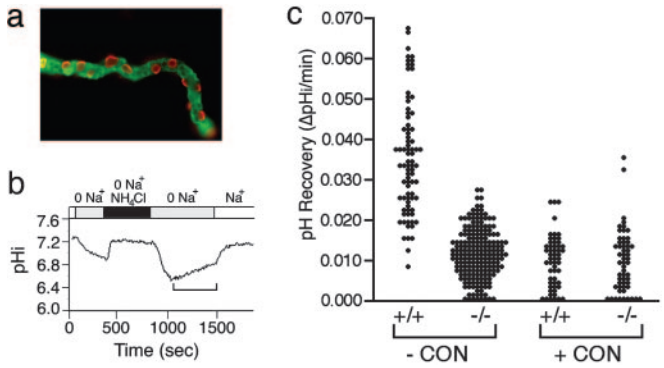

Fig. 4. Impaired proton secretion from single ICs of *Atp6v1b1*$^{-/-}$ mice after acute acidification. CD fragments were isolated and acidified as described in *Methods*, and the recovery of pH was measured in the presence or absence of concanamycin (CON). (*a*) ICs were identified on morphologic criteria; the ability to distinguish ICs was shown by staining for AE1 as in Fig. 2. (*b*) Measurement of recovery of intracellular pH after acute acidification. Cells were acidified with NH_4Cl, and recovery of intracellular pH was monitored with the pH-sensitive dye BCECF in the absence of Na^+ as described in *Methods*. The rate of recovery was determined from the slope of the increase in pH with time (bracket). (*c*) Distribution of rates of pH recovery in +/+ and −/− mice in the absence and presence of CON. Each data point represents the rate of recovery in a single cell. +/+ ICs show a markedly greater mean rate of recovery than cells from −/− mice ($P < 0.001$). CON inhibited recovery of pH in +/+ cells ($P < 0.001$) to a rate indistinguishable from that seen in −/− cells in the absence or presence of the drug.

Localization of the H$^+$ATPase B2-Subunit Is Altered in Atp6v1b1$^{-/-}$ Medulla. In addition to the B1 isoform, expression of the alternative B subunit isoform (B2) has also been detected in type A ICs of both rat and mouse, predominantly in a vacuolar pattern but also on the apical membrane (14). To determine whether expression and/or localization of the alternative B2-subunit of the H$^+$ ATPase is modified in *Atp6v1b1*$^{-/-}$ kidney, we performed immunohistochemistry using a B2-specific antibody (Fig. 5). Apical staining was rare in the cortex and outer stripe of *Atp6v1b1*$^{+/+}$, *Atp6v1b1*$^{+/-}$, and *Atp6v1b1*$^{-/-}$ outer medulla (data not shown). In *Atp6v1b1*$^{+/+}$ and *Atp6v1b1*$^{+/-}$ mice, apical B2-subunit staining was found in a small minority of cells in the inner stripe (data not shown) and in 14% cells from the inner medulla (IM) (Fig. 5*a*; 1,332 cells counted from three animals). In contrast, the proportion of apically staining cells in the IM increased to 74% in *Atp6v1b1*$^{-/-}$ mice (Fig. 5*b*; 704 cells counted from two animals).

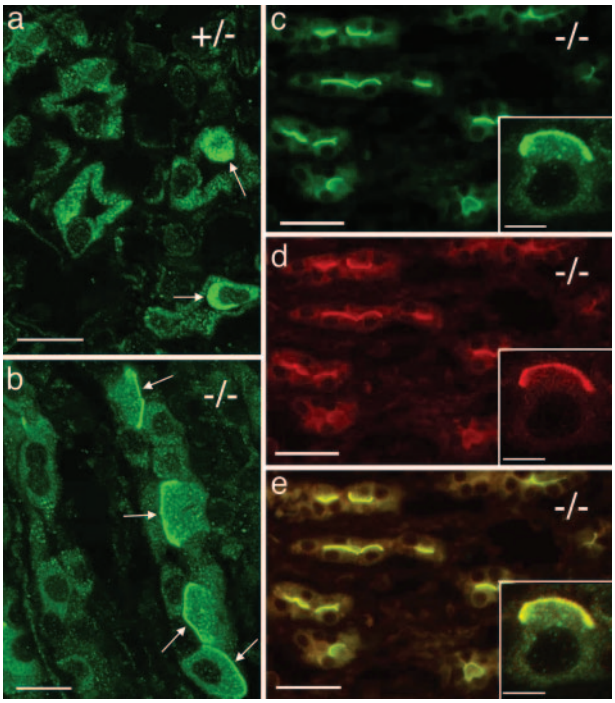

Fig. 5. Increased apical expression of the H$^+$ ATPase B2-subunit in *Atp6v1b1*$^{-/-}$ kidney. Kidney sections were stained for the B2-subunit and visualized as described in *Methods*. (*a*) B2 is predominantly cytoplasmic in +/− inner medullary collecting duct (IMCD). (*b*) B2 shows significant enhancement at the apical membrane in −/− IMCD. (*c–e*) Colocalization of B2 (green) with the H$^+$ ATPase E subunit (red) at the apical membrane of IMCD of −/− mice. (*Insets*) A single A-IC at higher magnification. (Scale bars, 15 μm in *a* and *b*, 30 μm in *c–e*, and 5 μm in *Insets*.)

To determine whether this apical B2-subunit colocalizes with other components of the H$^+$ ATPase complex, we compared the localization of the B2-subunit (Fig. 5*c*) with the E-subunit (Fig. 5*d*), another subunit of the H$^+$ ATPase (V1) domain known to redistribute from cytoplasmic vesicles to the apical plasma membrane of medullary ICs in response to chronic dietary acid loads (22). This B2 staining colocalized with the E-subunit in a narrow apical band at the surface of A-ICs of the IM (Fig. 5*e*), suggesting that B2-subunit incorporation in apical H$^+$ ATPases increases in the absence of functional B1-subunit.

Discussion

Genetic studies of humans have demonstrated that the H$^+$ ATPase B1-subunit is essential for the maintenance of normal systemic pH in humans on a normal diet (5). Our current results in mice demonstrate that the B1-subunit is essential for renal proton secretion induced by increased systemic or intracellular concentrations of protons, as well as the electrogenic proton secretion induced in response to furosemide infusion. The present data also indicate that proton pumps containing the B1-subunit mediate the majority of Na^+-independent intracellular pH recovery by ICs in the setting of an acute acid load. Taken together, these results suggest that the B1 isoform is the major B subunit isoform that incorporates into functional plasma membrane H$^+$ ATPases in ICs of the cortical CD and that these pumps are the primary mediators of the renal response to systemic metabolic acidosis.

Although human dRTA patients harboring homozygous B1-subunit mutations typically present as infants with spontaneous metabolic acidosis and failure to thrive (5), *Atp6v1b1*$^{-/-}$ mice raised on a standard rodent diet were healthy, grew normally, and did not develop metabolic acidosis. This phenotypic discrepancy is likely related to dietary differences. Standard rodent chow has been shown to provide a large net dietary alkali load (23), whereas the typical Western human diet, with its higher protein content, provides a net acid load (1). Because studies in both humans (24) and rats (25) have shown a positive correlation between increasing dietary protein intake and net acid excretion, proton secretion mediated by the B1-subunit may become essential for the maintenance of systemic pH homeostasis only in the context of a net dietary acid load. Nevertheless, the significant difference in urine pH indicates that the B1-subunit does play a role in mice on a standard diet.

A second difference between the phenotype of humans and mice deficient for Atp6v1b1 is the uniform hypercalciuria in humans (5), which is absent in the mouse. *Atp6v1b1*$^{-/-}$ mice had normal bone density, did not develop nephrocalcinosis, and, in fact, displayed significantly lower urine calcium excretion compared to WT. The absence of skeletal abnormalities in *Atp6v1b1*$^{-/-}$ mice supports the hypothesis that hypercalciuria in humans is attributable to dissolution of bone by the systemic acidosis, rather than a direct role of *Atp6v1b1* in bone metabolism. Our findings are consistent with the observation that B2, rather than B1, is the B-subunit expressed in osteoclasts (26).

Finally, study of *Atp6v1b1*$^{-/-}$ mice has yet to demonstrate an essential role for the B1-subunit in non-renal tissues known to express this protein in WT mice, such as male reproductive tract and inner ear. Although it has been proposed that H^+ ATPase activity in the male reproductive tract plays a role in fertility (16), male *Atp6v1b1*$^{-/-}$ mice were fertile. Although sensorineural hearing loss cosegregates with dRTA in kindreds harboring B1-subunit mutations (5), inner ear histology, auditory brainstem responses, and endocochlear potential were normal in *Atp6v1b1*$^{-/-}$ mice (27).

In the absence of the B1-subunit, we found a compensatory increase in apical H^+ ATPase complexes containing the B2-subunit in IM. Although the functional significance of this increased apical B2-subunit expression is uncertain, these results raise the possibility that, under some circumstances, the B2-subunit may provide partial functional compensation for the loss of the B1-subunit. Because *Atp6v1b1*$^{-/-}$ mice did achieve some increase in urinary acidification after oral acid challenge, apical B2-subunit-containing H^+ ATPase complexes could indeed be contributing to proton secretion in this setting, although not at a level sufficient to maintain normal pH homeostasis.

Whether the B1-subunit contributes to H^+ ATPases that mediate acidification of intracellular compartments such as endosomes and lysosomes has remained a matter of debate. Because *Atp6v1b1*$^{-/-}$ mice do not display evidence of generalized renal tubular dysfunction, our results suggest that the B1-subunit is unlikely to be required for endocytic acidification processes in renal epithelia.

The relative importance of plasma membrane H^+ ATPase activity compared to other acidification processes in the maintenance of pH homeostasis at the cellular and organismal level, both under normal dietary conditions, as well as in the setting of systemic acidosis, remains to be fully elucidated. Indeed, the fact that mice lacking the B1-subunit retain some degree of urinary acidification after oral acid challenge provides functional evidence for these alternative acidification processes. However, the fact that *Atp6v1b1*$^{-/-}$ mice develop a more severe metabolic acidosis than controls after oral acid loading indicates that these other acidification processes cannot fully compensate for loss of the B1-subunit. Our study of Na^+-independent pH_i recovery after acid loading suggests that these non-H^+ ATPase mechanisms mediate only a minor component of urinary acidification by ICs.

We thank M. Kashgarian for histological assessment; S. A. Mentone for tissue sectioning; G. Cameron for blood sample collection; and C. Nelson-Williams, Y. Lu, K. Choate, F. Karet, and T. Wang for helpful discussions. K.E.F. was an Investigator of the National Institutes of Health Medical Scientist Training Program. C.A.W. was a Feodor-Lynen fellow of the Alexander-von-Humboldt Foundation. M.A.B. was supported by the Wellcome Trust. T.G.P. was supported by a National Institutes of Health institutional training grant. This work was supported by grants from the National Institutes of Health (to J.P.G., G.G., D.B., and S.B.). R.P.L. is an Investigator of the Howard Hughes Medical Institute.

1. Gennari, F. J. & Maddox, D. A. (2000) in *The Kidney: Physiology and Pathophysiology*, eds. Seldin, D. W. & Giebisch, G. (Lippincott, Philadelphia), pp. 2015–2053.
2. DuBose, T. D. & Alpern, R. J. (2001) in *The Metabolic & Molecular Bases of Inherited Disease*, eds. Scriver, C. R., Beaudet, A. L., Sly, W. S. & Valle, D. (McGraw-Hill, New York), pp. 4983–5021.
3. Hamm, L. L. & Alpern, R. J. (2000) in *The Kidney: Physiology and Pathophysiology*, eds. Seldin, D. W. & Giebisch, G. (Lippincott, Philadelphia), pp. 1935–1979.
4. Karet, F. E., Gainza, F. J., Györy, A. Z., Unwin, R. J., Wrong, O., Tanner, M. J. A., Nayir, A., Alpay, H., Santos, F., Hulton, S. A., *et al.* (1998) *Proc. Natl. Acad. Sci. USA* **95,** 6337–6342.
5. Karet, F. E., Finberg, K. E., Nelson, R. D., Nayir, A., Mocan, H., Sanjad, S. A., Rodriguez-Soriano, J., Santos, F., Cremers, C. W., Di Pietro, A., *et al.* (1999) *Nat. Genet.* **21,** 84–90.
6. Smith, A. N., Skaug, J., Choate, K. A., Nayir, A., Bakkaloglu, A., Ozen, S., Hulton, S. A., Sanjad, S. A., Al-Sabban, E. A., Lifton, R. P., *et al.* (2000) *Nat. Genet.* **26,** 71–75.
7. Gluck, S. L., Underhill, D. M., Iyori, M., Holliday, L. S., Kostrominova, T. Y. & Lee, B. S. (1996) *Annu. Rev. Physiol.* **58,** 427–445.
8. Wagner, C. A., Finberg, K. E., Breton, S., Marshansky, V., Brown, D. & Geibel, J. P. (2004) *Physiol. Rev.* **84,** 1263–1314.
9. Stevens, T. H. & Forgac, M. (1997) *Annu. Rev. Cell. Dev. Biol.* **13,** 779–808.
10. Nishi, T. & Forgac, M. (2002) *Nat. Rev. Mol. Cell. Biol.* **3,** 94–103.
11. Nelson, R. D., Guo, X.-L., Masood, K., Brown, D., Kalkbrenner, M. & Gluck, S. (1992) *Proc. Natl. Acad. Sci. USA* **89,** 3541–3545.
12. Brown, D. & Breton, S. (2000) *J. Exp. Biol.* **203,** 137–145.
13. Finberg, K. E., Wagner, C. A., Geibel, J. P. & Lifton, R. P. (2003) *Gene* **318,** 25–34.
14. Păunescu, T. G., Da Silva, N., Marshansky, V., McKee, M., Breton, S. & Brown, D. (2004) *Am. J. Physiol.* **287,** C149–C162.
15. Wagner, C. A., Finberg, K. E., Stehberger, P. A., Lifton, R. P., Giebisch, G. H., Aronson, P. S. & Geibel, J. P. (2002) *Kidney Int.* **62,** 2109–2117.
16. Breton, S., Smith, P. J., Lui, B. & Brown, D. (1996) *Nat. Med.* **2,** 470–472.
17. Bailey, M. A., Giebisch, G., Abbiati, T., Aronson, P. S., Gawenis, L. R., Shull, G. E. & Wang, T. (2004) *J. Physiol.* **561,** 765–775.
18. Wagner, C. A., Lükewille, U., Valles, P., Breton, S., Brown, D., Giebisch, G. H. & Geibel, J. P. (2003) *Pflügers Arch.* **446,** 623–632.
19. Winter, C., Schulz, N., Giebisch, G., Geibel, J. P. & Wagner, C. A. (2004) *Proc. Natl. Acad. Sci. USA* **101,** 2636–2641.
20. Batlle, D. C. (1986) *Metabolism* **35,** 852–860.
21. Dröse, S., Bindseil, K. U., Bowman, E. J., Siebers, A., Zeeck, A. & Altendorf, K. (1993) *Biochemistry* **32,** 3902–3906.
22. Bastani, B., Purcell, H., Hemken, P., Trigg, D. & Gluck, S. (1991) *J. Clin. Invest.* **88,** 126–136.
23. Lin, S.-H., Cheema-Dhadli, C., Chayaraks, S., Chen, C.-B., Gowrishankar, M. & Halperin, M. L. (1998) *Am. J. Physiol.* **274,** F1037–F1044.
24. Remer, T. (2000) *Semin. Dialysis* **13,** 221–226.
25. Kharma, A., Simoni, J., Hacker, C., Duran, M.-J. & Wesson, D. E. (2004) *J. Am. Soc. Nephrol.* **15,** 2266–2275.
26. Lee, B. S., Holliday, S., Ojikutu, B., Krits, I. & Gluck, S. L. (1996) *Am. J. Physiol.* **270,** C382–C388.
27. Dou, H., Finberg, K. E., Cardell, E. L., Lifton, R. P. & Choo, D. (2003) *Hear. Res.* **180,** 76–84.